UNIVERSITÀ DEGLI STUDI DI BERGAMO
Department of Economics

WORKING PAPERS

Flight Delays, Operational Responses, and Their Environmental Cost: Evidence from European Skies

Andrea Gualini and Estelle Malavolti

November 2025 - WP N. 33 Year 2025

Working papers – Department of Economics
n. 33

Flight Delays, Operational Responses, and Their Environmental Cost: Evidence from European Skies

Andrea Gualini, Estelle Malavolti

Università degli Studi di Bergamo
2025

Flight Delays, Operational Responses, and Their Environmental Cost: Evidence from European Skies / Andrea Gualini, Estelle Malavolti - Bergamo: Università degli Studi di Bergamo, 2025.
Working papers of Department of Economics, n. 33
ISSN: 2974-5586
DOI: 10.13122/WPEconomics_33

Progetto grafico: Servizi Editoriali – Università degli Studi di Bergamo
Università degli Studi di Bergamo
via Salvecchio, 19
24129 Bergamo
Cod. Fiscale 80004350163
P. IVA 01612800167

https://aisberg.unibg.it/handle/10446/313206

Flight Delays, Operational Responses, and Their Environmental Cost: Evidence from European Skies

Andrea Gualini[†] and Estelle Malavolti[‡]

[†]University of Bergamo, Italy
[‡]Toulouse School of Economics & ENAC, France
[†]andrea.gualini@unibg.it
[‡]estelle.malavolti@enac.fr

November 2025

Abstract

This paper investigates the operational and environmental consequences of flight delays in the European airline industry. Using detailed 2023 data on aircraft rotations, we develop three complementary empirical models. The first quantifies *within-flight mitigation*, capturing how airlines strategically absorb departure delays through en-route and destination-side adjustments. The second examines *delay propagation* across consecutive flights, shedding light on the effectiveness of turnaround buffers and network-level externalities. The third links airborne delays to fuel consumption and CO_2 emissions, providing a quantitative estimate of the environmental costs of tactical recovery strategies. Our findings show that within-flight mitigation absorbs roughly 5% of departure delays, propagation across rotations is moderate, and each additional airborne minute increases fuel burn by roughly 22 kg and CO_2 emissions by 71 kg. From a policy and management perspective, these results underscore the importance of realistic scheduling, buffer allocation, and coordination between airlines and air traffic control to improve punctuality and reduce environmental impacts, highlighting trade-offs central to airline operational and industrial strategy.

Keywords: Delay mitigation, CO_2 emissions, EU airlines, Air transport policy

1 Introduction

Delays represent a large amount of time and money. In Europe, in one year, the cumulated delays represent more than hundreds of years. Moreover, around 30% of the flights in Europe are delayed by more than 15 min. However, not every single delay has the same impact. Even today, despite continuous improvements in airline operations and in the systems managing air traffic, delays remain a major issue affecting service quality. On the one hand, they generate substantial additional costs for airlines (aircraft repositioning, network externalities, crew scheduling, etc.); on the other hand, they may reduce passengers' confidence in the reliability of carriers after repeated negative experiences.

Hence, understanding the causes and consequences of delays is of central importance for airlines.

The main research question of this paper is how airlines' tactical adjustments to delays affect flight operations and the environment, particularly in terms of CO_2 emissions, while also exploring delay propagation and mitigation mechanisms.

We develop a gradual empirical methodology based on three complementary models. First, using data on European traffic, we analyse how departure delays influence variations in flight time, and how arrival delays are affected by the actual flight time. This first model captures the *mitigation effect*, i.e. how airlines strategically adjust flight operations to compensate for a pre-existing departure delay. The analysis of this mitigation behaviour has also received growing attention in the IO literature (Forbes et al. (2019)).

The second model focuses on the *propagation effect*, relating the departure delay of an aircraft to the late arrival of its inbound flight. Understanding this propagation mechanism is crucial to assessing network externalities and the extent to which airlines internalise them. The analysis of propagation delays has always received much attention in the literature with both theoretical and empirical contributions (Brueckner (2002a), Brueckner (2002b), Brueckner (2005), Brueckner et al. (2021), Brueckner et al. (2022), Bubalo and Gaggero (2021)).

Brueckner et al. (2025) have developed transparent measures for identifying propagated delays (e.g., a propagated departure delay occurs when the inbound arrival delay exceeds the scheduled ground buffer). They quantify how schedule buffers affect arrival delays using flight-sequence data from U.S. government sources. More structural approaches also exist, such as Kafle and Zou (2016), who propose a joint analytical–econometric model decomposing delays into (i) newly formed (exogenous) and (ii) propagated components, and estimate how much of each minute of new delay carries over to subsequent flights. Their framework explicitly accounts for ground buffers, providing interpretable coefficients that directly map into operational performance.

A more recent contribution by Dou et al. (2024) introduces a hybrid structural–machine-learning framework that estimates a weighted, directed graph of delay propagation across an airline's network. Their work emphasises identification conditions for interpreting propagation coefficients as causal effects and uses large operational datasets to estimate airline-specific propagation networks.

Finally, the third model developed in this paper links airlines' strategic reactions to CO_2 emissions. Among the short-run operational measures available to airlines is to increase cruising speed, which reduces airborne delay but raises fuel consumption and thus emissions relative to the scheduled flight plan. Intuitively, when ex ante measures such as schedule buffers or aircraft repositioning are insufficient, these ex post strategies may have adverse environmental consequences.

While the relationship between flight delays and CO_2 emissions has received limited attention so far, a few related contributions exist, altough typically confined to specific contexts or operational phases: Chen et al. (2017) and Huang et al. (2020) analyse the joint efficiency and productivity of airlines accounting for both CO_2 emissions and delays, but without explicitly modelling their causal interaction. Dissanayaka et al. (2020), focus more narrowly on the taxiing phase, estimating the emission impact of ground delays at a single airport). To the best of our knowledge, no comprehensive empirical analysis has systematically linked airborne delay management to emission outcomes.

Our paper complements these analyses by examining more deeply the *within-flight mitigation* of delays, an aspect that has so far received limited empirical attention com-

pared to the ripple effect in the network. Building on European data, we develop a gradual empirical strategy based on three complementary models designed to disentangle the underlying mechanisms. The first model provides a detailed exploration of airlines' short-run tactical adjustments within flights, while the second model serves more as a validation exercise, offering an updated picture of delay propagation and recovery patterns in the European market as of 2023. The third model introduces the main novelty of this study, linking these operational responses directly to fuel consumption and CO_2 emissions by explicitly connecting delay management to fuel-intensive recovery actions within flights. By estimating how airborne delay and its mitigation affect fuel and CO_2 consumption, we quantify the environmental costs of airlines' short-run responses to schedule disruptions. In doing so, the paper extends existing research providing new empirical evidence on the behavioural and environmental dimensions of delay management in commercial aviation - a perspective largely absent from previous studies.

The remainder of the paper is structured as follows. Section 2 presents the dataset and defines the main variables. Section 3 introduces the econometric models, Section 4 discusses the results. Section 5 concludes.

2 Data, Variables and Descriptive Statistics

2.1 Data Sources

The empirical analysis combines multiple datasets related to flight operations, emissions, and schedule characteristics, primarily sourced from the suite of OAG databases for 2023. These include the Flight Status Data (On-Time Performance, OTP), which records scheduled and actual times for departure, arrival, taxi-out, taxi-in, and airborne segments; the Emissions Data, which provides estimates of fuel burn and CO_2 emissions per flight and stage; the Schedule Analyser (SA), which contains scheduled flight characteristics such as aircraft model, seating capacity, flight frequency, and operator identifiers; and the Traffic Analyser (TA), which offers market and passenger data such as codeshare flags and ticket prices. Unlike the other datasets, the Traffic Analyser data is available on a monthly basis.

Additional auxiliary data (BADA/NEST trajectory and airspace management information, and meteorological variables) will be used for validation through a case study. The working sample focuses on flights within Western Europe, covering fifteen countries. Routes affected by airspace closures related to the war in Ukraine are excluded to ensure comparability of operational conditions.[1]

2.2 Sample and Structure

The unit of observation is a single scheduled flight leg, defined from gate-out to gate-in. A panel is constructed by indexing each observation by aircraft tail number and day, allowing the tracking of the same aircraft across its daily rotation. This structure makes it possible to analyse both within-flight delay absorption and across-flight delay propagation for the same aircraft.

Tables 1 and 2 provide illustrative examples of how the dataset follows the sequence of flights operated by individual aircraft over the course of a day.

[1] List of countries in Table 8 in the Appendix

Table 1 reports, for two specific tail numbers, the succession of legs and the corresponding departure, airborne, and arrival delays. The example shows how small initial delays (e.g., 1 minute at departure for the first leg of tail 9ABTI) can accumulate or be partially recovered in the air, and how larger delays later in the day (such as 90 minutes before the last leg) may reflect the cascading effects of previous disruptions. Comparing the two aircraft-one operating medium-haul routes (e.g. CDG–LIS) and the other shorter intra-European segments-already suggests that propagation mechanisms may vary with route structure and daily scheduling intensity.

Table 2 decomposes the total gate-to-gate time for the same flights into its operational phases: taxi-out, take-off, climb-out, cruise, approach, and taxi-in-offering a more detailed view of where delays materialise. Examining the different rotations of the two aircraft shows how the duration of each phase can vary throughout the day and how crews sometimes mitigate accumulated delays by slightly adjusting airborne time (negative airborne delays), even though such recovery rarely offsets total arrival delays entirely.

Together, these examples help illustrate the panel structure of the analysis-where each aircraft-day sequence forms an observation unit-and provide an intuitive understanding of how delays can emerge and propagate along an aircraft's daily operations within Western Europe.

Table 1: Example of Aircraft Rotations and Delay Components (minutes)

Sched Departure	TailNumber	AirportPair	Sequence	Departure Delay	Arrival Delay	Airborne Delay
01/01/2023 06:10	9ABTI	CDG-FCO	1	1	10	9
01/01/2023 09:10	9ABTI	FCO-CDG	2	28	26	-2
01/01/2023 12:30	9ABTI	CDG-LIS	3	45	61	16
01/01/2023 16:10	9ABTI	LIS-CDG	4	90	61	-29
01/01/2023 06:25	9HQDD	FCO-PMO	1	0	5	5
01/01/2023 09:45	9HQDD	PMO-VLC	2	0	12	12
01/01/2023 12:20	9HQDD	VLC-FCO	3	18	10	-8

Table 2: Example of Aircraft Rotations and Associated CO_2 Emissions (tonnes)

Sched Departure	TailNumber	Taxi Out	Takeoff	Climbout	Cruise	Approach	Taxi In	Total
01/01/2023 06:10	9ABTI	1.27	0.31	0.77	10.92	0.50	0.43	14.20
01/01/2023 09:10	9ABTI	1.02	0.31	0.78	10.83	0.50	0.68	14.12
01/01/2023 12:30	9ABTI	0.78	0.30	0.75	17.77	0.49	0.17	20.24
01/01/2023 16:10	9ABTI	0.47	0.34	0.86	14.51	0.56	0.47	17.21
01/01/2023 06:25	9HQDD	0.98	0.32	0.82	4.49	0.50	0.21	7.33
01/01/2023 09:45	9HQDD	1.43	0.32	0.82	11.60	0.50	0.29	14.97
01/01/2023 12:20	9HQDD	0.37	0.32	0.82	11.34	0.50	0.41	13.76

2.3 Variable Definitions

Three complementary measures of delay are defined for each flight. *DEPDELAY* is the difference between the actual off-block time and the scheduled departure time. *ARRDELAY* is the difference between the actual on-block time and the scheduled arrival time. *AIRDELAY* measures the deviation between the actual time spent in the air and the scheduled, or padded, airborne time.

Each delay measure is expressed in minutes. Departure and arrival delays capture deviations relative to the scheduled gate times, while airborne delay isolates the in-flight component.

These measures are defined net of the buffers already embedded in airline schedules. Airlines typically include ground buffers through longer scheduled taxi-out or taxi-in times, and air buffers through inflated scheduled airtime relative to the minimum required. The delay variables therefore capture only the unexpected deviations beyond these planned buffers.

Specifically, *DEPDELAY* represents the residual departure delay not absorbed by scheduled turnaround slack; *AIRDELAY* measures deviations in the air relative to padded airtime; and *ARRDELAY* reflects the residual delay at arrival after both airborne and ground recovery.

For the propagation models, a variable *LAGDELAY* is also constructed, defined as the arrival delay of the previous flight operated by the same aircraft on the same day. While *DEPDELAY*, *AIRDELAY*, and *ARRDELAY* allow us to assess the transmission mechanisms within each individual flight, *LAGDELAY* captures the potential transmission of delays across rotations.

2.4 Descriptive Statistics

Table 3 reports descriptive statistics for the main delay and emissions variables, while Table 4 summarises the main control variables used in the econometric models. All variables are defined at the flight-leg level.

Table 3: Summary of Main Variables

Variable	Obs	Mean	Std. Dev.	Min	Max
ARRDELAY (minutes)	1,156,815	21.92	33.21	-223	1,556
DEPDELAY (minutes)	1,156,815	24.59	32.11	-219	1,564
AIRDELAY (minutes)	1,156,815	-0.96	15.88	-115	1,414
LAGDELAY (minutes)	1,156,815	7.59	25.55	-194	1,434
FUEL (tonnes)	1,156,815	3.56	2.01	0.28	39.1
CO2 (tonnes)	1,156,815	11.26	6.36	0.87	123.3

Table 4: Summary of Control Variables

Variable	Obs	Mean	Std. Dev.	Min	Max
ROUTE_NUMCOMP	1,156,815	1.56	0.77	1	5
ROUTE_MKT_SHARE	1,156,815	0.36	0.30	0.01	1
CODESHARE	1,156,815	0.71	0.45	0	1
EARLYMORNING	1,156,815	0.05	0.24	0	1
MORNING	1,156,815	0.30	0.46	0	1
AFTERNOON	1,156,815	0.32	0.46	0	1
EVENING	1,156,815	0.33	0.47	0	1
DOMESTIC	1,156,815	0.35	0.48	0	1
DISTANCE (Km)	1,156,815	509	315	102	2,561
LCC	1,156,815	0.24	0.43	0	1
ALLIED	1,156,815	0.73	0.44	0	1
IS_HUB	1,156,815	0.24	0.43	0	1
NUM_FLIGHTS_OUT_APT_DH	1,156,815	7.52	6.29	1	33
NUM_FLIGHTS_IN_APT_DH	1,156,815	7.81	6.86	1	40

Average *ARRDELAY* and *DEPDELAY* are of similar magnitude, around twenty to twenty-five minutes, while mean *AIRDELAY* is slightly negative, indicating that actual airtime is often shorter than scheduled. This reflects the widespread inclusion of airtime buffers by airlines. Fuel burn and CO_2 emissions (*FUEL* and *CO2*) show considerable heterogeneity across routes, mainly explained by distance and aircraft type. Control variables display expected variation: route distance ranges from about one hundred to over two thousand five hundred kilometres, and approximately one quarter of flights are operated by low-cost carriers.

These statistics confirm that most scheduled flights include significant pre-built slack, yet residual delays remain frequent. The observed variation in delay and emissions outcomes provides sufficient within-aircraft variation to identify both delay mitigation mechanisms and environmental effects in the econometric analysis.

2.5 Descriptive Insights

This subsection provides descriptive evidence on delay patterns across airlines, routes, and time dimensions within Western Europe. The figures below summarise the main stylised facts that motivate the econometric analysis while offering a broad picture of delay dynamics across Western Europe

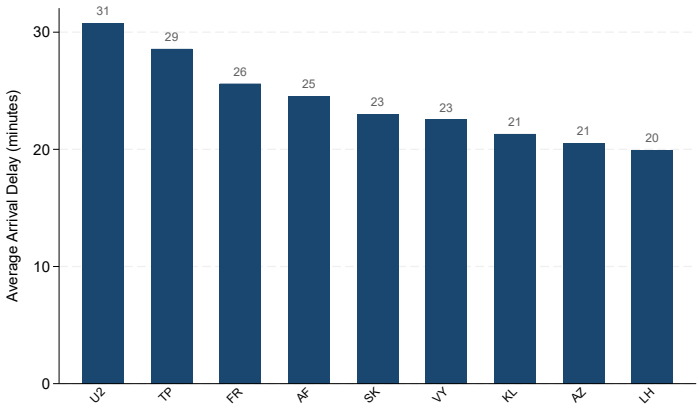

Figure 1: Top 10 European Airlines by Average Arrival Delay

Average *ARRDELAY* differs widely among the top European carriers[2] Network carriers tend to experience moderate delays, potentially benefiting from greater operational flexibility - such as the ability to reassign aircraft or reroute passengers across their hub-and-spoke networks (Bubalo and Gaggero (2021)) - while several low-cost carriers display higher mean arrival delays, reflecting tighter schedules and greater aircraft utilisation. This cross-airline variation highlights the relevance of controlling for carrier-specific characteristics in the econometric framework.

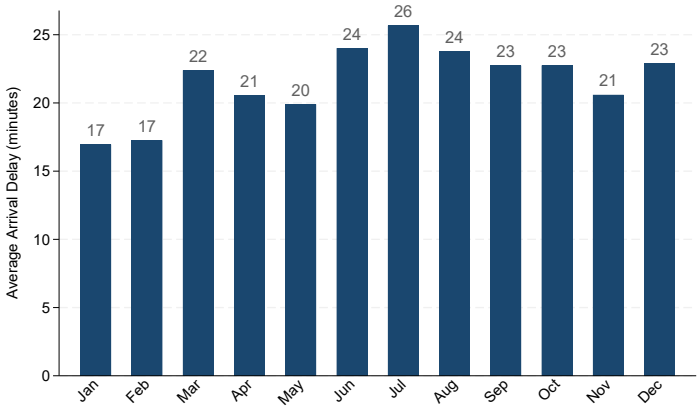

Figure 2: Average Arrival Delay by Month

Delays peak during the summer months (June to August), when traffic demand is highest, and rise again slightly in December due to both winter operations and the ongoing demand peak. The pattern closely follows the seasonal cycle of European air traffic demand.

[2]see Table 9 in the Appendix for the full list

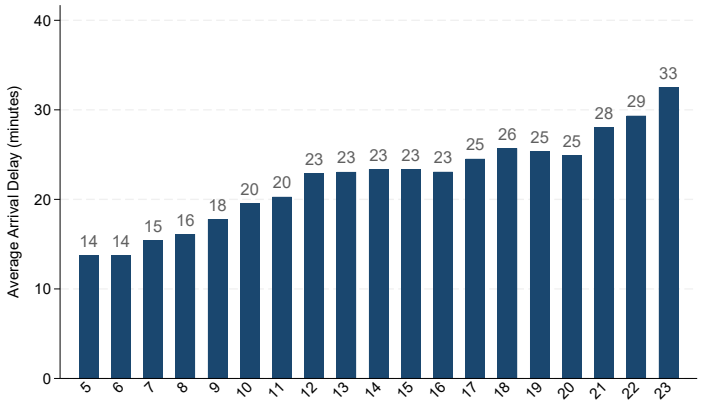

Figure 3: Average Arrival Delay by Hour of Departure

Delays accumulate throughout the day. Flights departing early in the morning tend to arrive on time, whereas those leaving in the late afternoon or evening are more affected by propagated delays from earlier rotations. This intra-day build-up underscores the importance of turnaround buffers and propagation mechanisms examined later in the paper.

Overall, three patterns emerge. First, delays are heterogeneous across airlines and routes. Second, they exhibit marked seasonal cycles. Third, congestion and rotation effects cause delays to intensify later in the day. These descriptive insights, specific to Western European operations, highlight the structural congestion and propagation mechanisms characterising the region's airspace and provide useful guidance and motivation for the empirical analysis developed in Section 3.

3 Empirical Models

This section translates conceptual models into estimable econometric specifications. We define the main variables and indexing structure, present the three families of regressions (within-flight mitigation, cross-flight propagation, and environmental impacts) and discuss issues of identification, estimation, and measurement.

3.1 Data Structure and Observational Unit

Each observation corresponds to a flight leg operated by aircraft tail–day unit p on route r (origin–destination pair) and belonging to airline a, in sequence position s within the same-day rotation. Variables are thus indexed by $pras$, allowing us to track delay dynamics both within a given flight and across consecutive legs of the same aircraft on a given operational day.

The key outcome variables, as reported in Table 3 are: *DEPDELAY*, the off-block departure delay in minutes; *AIRDELAY*, the airborne delay, defined as the difference between actual airborne time and an uncongested baseline; *ARRDELAY*, the on-block arrival delay; *LAGDELAY*, the arrival delay of the previous leg operated by the same aircraft tail on the same day, which captures delay propagation across rotations; *FUEL*, the block fuel consumption in tonnes; and *CO2*, the corresponding block CO_2 emissions in tonnes.

The vector of control variables $\mathbf{X}_{pras}$ are reported in Table 4, and includes route, schedule, and airport-level characteristics that capture structural and temporal heterogeneity in flight operations. Specifically, it contains the number of competitors on the route (*ROUTE_NUMCOMP*) or, alternatively, the airline's market share on that route (*ROUTE_MKT_SHARE*), a codeshare indicator (*CODESHARE*), and time-of-day dummies distinguishing early morning, morning, afternoon, and evening departures. Additional controls include a domestic-route dummy (*DOMESTIC*), great-circle distance in kilometres (*DISTANCE*), a low-cost carrier indicator (*LCC*), an alliance membership indicator (*ALLIED*), and a hub-airport dummy (*IS_HUB*). Airport activity is proxied by the number of departures from the origin airport and arrivals at the destination airport within the same hour (*NUM_FLIGHTS_OUT_APT_DH* and *NUM_FLIGHTS_IN_APT_DH*).

All specifications share a common set of control variables, fixed effects, and an idiosyncratic error term. For compactness, we define

$$\mathcal{C}_{pras} \equiv \mathbf{X}_{pras}\Gamma + \alpha_p + \delta_r + \eta_a + \varepsilon_{pras},$$

where $\mathbf{X}_{pras}$ collects the control variables listed in Table 4, α_p denote aircraft–day fixed effects, δ_r route fixed effects, η_a airline fixed effects, and ε_{pras} is the idiosyncratic error term. The aircraft–day effects absorb all daily operational variation such as weather conditions or shocks constant within the same day, the route effects capture time-invariant characteristics of each origin–destination airport pair, and the airline effects control for carrier-specific factors.[3]

This structure exploits within-aircraft-day variation across routes and flights, making additional temporal dummies (e.g., day-of-week or month) redundant. Standard errors are two-way clustered by aircraft tail and airline. All subsequent equations are expressed in reduced form as outcome–predictor relationships plus $\mathcal{C}_{pras}$.

3.2 Model 1: Within-Flight Delay Relationships

We begin by analysing how delays are absorbed within a single gate-to-gate operation, considering adjustments made before pushback, during the flight, and after landing. The following specifications quantify how departure delays are transmitted to subsequent operational stages.

The first specification examines the gate-to-gate relationship between departure and arrival delays:

$$ARRDELAY_{pras} = \beta_1 \, DEPDELAY_{pras} + \mathcal{C}_{pras}. \tag{1}$$

The coefficient β_1 represents the gate-to-gate delay pass-through, while the share of delay absorbed within the leg is given by $1 - \beta_1$.

To isolate the role of post-landing operations, the second equation relates arrival delay to airborne delay:

$$ARRDELAY_{pras} = \beta_2 \, AIRDELAY_{pras} + \mathcal{C}_{pras}. \tag{2}$$

Here, β_2 captures how airborne delay translates into arrival delay, with $1 - \beta_2$ indicating average recovery achieved on the ground at destination.

[3]As a robustness check, we additionally include route–tail fixed effects, which absorb any time-invariant characteristics specific to a given aircraft repeatedly operating a given route-such as persistent scheduling patterns, aircraft-route matching, or structural operational constraints. This ensures that our results are not influenced by stable heterogeneity at the aircraft-route level. The main estimates remain essentially unchanged.

Finally, the third specification focuses on the en-route phase, linking airborne delay to departure delay:

$$AIRDELAY_{pras} = \beta_3 \, DEPDELAY_{pras} + \mathcal{C}_{pras}. \tag{3}$$

The coefficient β_3 measures the proportion of departure delay that persists during flight, while $1 - \beta_3$ reflects the degree of en-route recovery.

The three coefficients capture pass-through at different stages: gate-to-gate (β_1), destination-ground conditional on airborne delay (β_2), and en-route conditional on departure delay (β_3).

Taken together, these three dimensions form a coherent decomposition of how delays materialise and are managed within a flight. Analysing gate-to-gate, en-route, and destination-ground pass-through separately is essential because each stage is governed by distinct operational levers (pushback sequencing and ground handling, speed and routing choices in the air, taxi-in and gate availability upon arrival) and subject to different physical and regulatory constraints. By isolating the mechanisms of persistence and recovery in each phase, the model not only quantifies overall delay absorption, but also identifies where in the operation airlines have the greatest ability - or the most binding limits - to mitigate delays. This granular perspective is crucial for understanding operational efficiency, pinpointing bottlenecks, and linking tactical decisions to broader system-wide impacts studied in the subsequent models.

3.3 Model 2: Delay Propagation Across Flights

The second set of models investigates how delays propagate across consecutive legs operated by the same aircraft within a day, focusing on recovery between rotations.

The first specification relates departure delay to the delay of the previous arrival:

$$DEPDELAY_{pras} = \beta_4 \, LAGDELAY_{pras} + \mathcal{C}_{pras}. \tag{4}$$

The coefficient β_4 measures the proportion of inbound delay transmitted to the subsequent departure, while $1 - \beta_4$ captures the effectiveness of turnaround buffers and ground recovery at the origin.

A broader measure of propagation is obtained by linking arrival delay to the previous arrival delay:

$$ARRDELAY_{pras} = \beta_5 \, LAGDELAY_{pras} + \mathcal{C}_{pras}. \tag{5}$$

In this case, β_5 represents the end-to-end propagation factor, encompassing delay transmission through all operational stages of the subsequent leg.

An intermediate specification links airborne delay to the previous arrival delay:

$$AIRDELAY_{pras} = \beta_6 \, LAGDELAY_{pras} + \mathcal{C}_{pras}. \tag{6}$$

The coefficient β_6 reflects the delay remaining at top-of-descent, after accounting for both ground recovery and potential en-route adjustments.

Taken together, the three coefficients provide a dynamic picture of how an inbound disruption evolves across rotations, tracing its progression through ground handling, the en-route phase, and the subsequent arrival. By separating propagation into these stages, the model identifies where airlines are most successful-or most constrained-in mitigating delays. The comparison between β_4, β_6, and β_5 is particularly informative: a small β_4

indicates substantial recovery during turnaround; if $\beta_6 < \beta_4$, additional catch-up occurs en route; and if β_5 remains sizeable, residual delays still carry through to the next arrival despite both margins of adjustment. This decomposition clarifies the mechanisms that stabilise operations and those that amplify disruptions, offering a clear view of operational bottlenecks, recovery margins, and overall resilience within the aircraft-day sequence.

3.4 Model 3: Environmental Impacts of Airborne Delays

The third model quantifies the environmental impact of deviations in airborne time-whether longer or shorter than scheduled-by relating airborne delay to fuel consumption and CO_2 emissions. Unlike Models 1 and 2, which characterise how delays arise and propagate, this specification focuses on the operational and environmental consequences of adjustments made in the air. Importantly, airborne delays may be either positive or negative, and the resulting fuel and emissions effects are not necessarily symmetric. Longer airborne times typically raise fuel burn through extended cruise, holding, or path stretching, but shorter airborne times do not always generate proportional savings. Early arrivals, for example, may result from pilot-initiated speed-ups, which increase fuel burn despite reducing time in the air, whereas favourable winds or direct routings can simultaneously shorten flight time and lower fuel use. This heterogeneity implies that positive and negative airborne delays reflect distinct operational mechanisms with different environmental implications.

Fuel consumption is modelled as:

$$\text{FUEL}_{pras} = \beta 7 \text{AIRDELAY}_{pras} + \mathcal{C}_{pras}. \tag{7}$$

The parameter β_7 captures the marginal change in fuel burn associated with one extra minute of airborne time, reflecting the combined effects of altered cruise duration, speed adjustments, tactical rerouting, and holding patterns.

CO2 emissions are estimated analogously:

$$\text{CO2}_{pras} = \beta_8 \text{AIRDELAY}_{pras} + \mathcal{C}_{pras}. \tag{8}$$

The coefficient β_8 provides the corresponding marginal effect on emissions.[4]

By estimating both relationships directly, the model translates operational inefficiencies or tactical adjustments into environmental terms, allowing us to quantify the carbon and fuel implications of airborne time deviations-whether induced by upstream delays, weather conditions, or air traffic management constraints.

Finally, disentangling the heterogeneous mechanisms behind positive and negative airborne delays would require high-resolution trajectory data (e.g., FMS or ADS-B with vertical profiles), detailed en-route weather fields, and sector-level ATC flow management information. Because such data are difficult to obtain at scale, a full identification of these channels is left for future research.

[4]In our dataset, CO_2 emissions are provided directly by OAG and are mechanically derived from fuel burn using the standard conversion factor $\kappa = 3.16$ tCO_2/t fuel. Consequently, β_8 and β_7 are mechanically linked through $\beta_8 = \kappa\beta_7$. We nonetheless report both coefficients for completeness and to allow more direct comparability with settings where emissions are independently measured or modelled.

3.5 Identification and Estimation

Identification in all models relies on the panel structure defined by aircraft tail numbers and their daily rotations. For the within-flight specifications (eqs. (1) to (3)), identification is obtained from variation in delays across operational phases for the same aircraft, on the same day, serving the same route. Aircraft–day, route, and airline fixed effects absorb all persistent or slowly varying heterogeneity: α_p captures daily operational conditions specific to each tail (e.g., weather, crew, maintenance), δ_r controls for time-invariant route characteristics, and η_a accounts for carrier-specific operational practices.

The propagation specifications (eqs. (4) to (6)) exploit the sequential structure of aircraft rotations. Conditional on fixed effects and controls, *LAGDELAY* acts as a quasi-predetermined shock to the next leg's timing, as it is inherited from the previous flight and unrelated to contemporaneous shocks affecting the subsequent leg. Identification therefore rests on within-aircraft-day variation across the rotation sequence.

All models include a rich set of control variables $\mathbf{X}_{pras}$ (summarised in Table 4) to absorb structural and temporal heterogeneity in flight operations. These cover route structure (e.g., number of competitors or airline market share, *CODESHARE*), temporal scheduling (time-of-day dummies), market type (*DOMESTIC*), physical and operational characteristics (*DISTANCE*, *LCC*, *ALLIED*, *IS_HUB*), and airport activity using hourly departures and arrivals at origin and destination. All specifications share the common structure introduced earlier through $\mathcal{C}_{pras}$.

Standard errors are clustered by aircraft tail and airline, as shocks may be correlated across flights operated by the same aircraft and within carriers, violating independence assumptions if not accounted for. Alternative clustering structures - such as clustering by aircraft tail and day - have been tested and do not materially affect the significance of the estimated coefficients. Baseline specifications are complemented by robustness checks and extended models. These assess heterogeneity in delay transmission across routes, test whether pass-through varies with the magnitude of the initial delay, and explore whether a flight's position in the rotation (e.g., feeder versus terminating leg) affects propagation dynamics. These analyses confirm that the identification strategy is stable across specifications and that core results are not driven by modelling choices or sample selection.

4 Results

This section presents the main econometric findings corresponding to the three models introduced above. The results quantify how delays are mitigated within flights and across aircraft rotations, and how these operational adjustments affect fuel consumption and CO_2 emissions.

4.1 Model 1: Within-Flight Delay Relationships

Table 5 presents a summary of the within-flight relationships between departure, airborne, and arrival delays. Only the main coefficients are shown; full regression tables for Models 1–3 are available upon request.

Departure delays are strongly transmitted to arrival delays, but the estimated coefficient $\hat{\beta}_1 \approx 0.95$ indicates that around 5% of the initial departure delay is recovered

Table 5: Within-Flight Delay Relationships

Dep. Variables.	(1) *ARRDELAY*	(2) *ARRDELAY*	(3) *AIRDELAY*
DEPDELAY	0.9464***		-0.0536***
	(0.0062)		(0.0062)
AIRDELAY		0.8040***	
		(0.0447)	
Observations	1,090,570	1,090,570	1,090,570
Adj. R-squared	0.8769	0.5501	0.1619
Tail–day FE	✓	✓	✓
Route FE	✓	✓	✓
Airline FE	✓	✓	✓
Robust standard errors in parentheses			
**** p<0.01, ** p<0.05, * p<0.1*			

within the same flight. This recovery arises through two complementary channels: en-route mitigation, where pilots may increase cruise speed or obtain more direct routings from Air Traffic Control to reduce airborne delay; and ground-level mitigation at destination, where shorter taxi-in times, priority runway exits, or expedited gate procedures help absorb residual delay upon arrival.

When arrival delay is regressed on airborne delay, the estimated coefficient $\hat{\beta}_2 \approx 0.80$ suggests that approximately 20% of airborne delay is absorbed before gate-in, confirming the role of destination-side mitigation. Overall, these results show that airlines and ATC actors can recover part-but not all-of a late departure, even after accounting for padded block times embedded in schedules.

4.2 Model 2: Delay Propagation Across Flights

Table 6 presents the results for delay propagation within aircraft rotations.

Table 6: Delay Propagation Across Flights

Dep. Variables.	(1) *DEPDELAY*	(2) *ARRDELAY*	(3) *AIRDELAY*
LAGDELAY	0.2109***	0.1329***	-0.0780***
	(0.0302)	(0.0339)	(0.0058)
Observations	697,799	697,799	697,799
Adj. R-squared	0.5485	0.5213	0.1947
Tail–day FE	✓	✓	✓
Route FE	✓	✓	✓
Airline FE	✓	✓	✓
Robust standard errors in parentheses			
**** p<0.01, ** p<0.05, * p<0.1*			

Arrival delays from one leg spill over to subsequent departures, but the magnitude of this propagation is moderate. The coefficient on lagged arrival delay in the departure-

delay equation is $\hat{\beta}_4 \approx 0.21$, implying that roughly one-fifth of an inbound delay persists to the next departure. The effect on the subsequent arrival delay is smaller, $\hat{\beta}_5 \approx 0.13$, indicating partial absorption of shocks across rotations. Moreover, the negative coefficient on lagged delay in the airborne-delay regression ($\hat{\beta}_6 < 0$) suggests that aircraft tend to fly slightly faster when starting behind schedule, consistent with tactical "catch-up" behaviour.

Propagation is thus limited: combining all mechanisms, about 80–90% of the previous delay is absorbed through scheduled turnaround buffers, ground-handling acceleration, and en-route speed adjustments. These results highlight the importance of buffer design-tight turnarounds amplify the risk of systemic delay, while generous buffers help contain shocks at the cost of lower utilisation.

4.3 Model 3: Fuel and CO_2 Impacts of Delays

Table 7 reports the estimated relationships between airborne delay and environmental outcomes.

Table 7: Fuel and CO_2 Impacts of Delays

Dep. Variables.	(1) *FUEL*	(2) *CO2*
AIRDELAY	0.0223***	0.0706***
	(0.0009)	(0.0029)
Observations	1,069,359	1,069,359
Adj. R-squared	0.99	0.99
Tail–day FE	✓	✓
Route FE	✓	✓
Airline FE	✓	✓
Robust standard errors in parentheses		
**** p<0.01, ** p<0.05, * p<0.1*		

Each additional minute of airborne time increases average fuel burn by approximately 22 kg and CO_2 emissions by approximately 71 kg per flight. Conversely, when flights experience negative airborne delays (i.e., spend less time aloft), fuel consumption and emissions decline proportionally. These results primarily reflect differences in actual flight duration - such as holding patterns, reroutings, and weather-related inefficiencies - rather than deliberate acceleration.

Episodes of "speed-up" to recover time have only a minor impact on total fuel use: the typical cruise-speed increase effect from pilots acceleration is small and often offset by favourable winds or ATC shortcuts. Nevertheless, given the large number of delayed flights across the network, even modest per-minute effects aggregate to substantial system-wide CO_2 implications.

5 Final Remarks and Conclusions

5.1 Main Insights

This paper has analysed how airlines in Western Europe manage delays within flights, across daily rotations, and how these operational responses translate into environmental impacts. Three main insights emerge.

First, within-flight mitigation is effective but limited. Consistent with the estimates in Model 1, only about 5% of departure delay is typically recovered before gate-in, despite the presence of padded block times. Both en-route and destination-ground adjustments contribute to this effect, but neither margin is large enough to offset most initial departure disruptions.

Second, delay propagation across rotations is moderate. Model 2 shows that roughly one-fifth of an inbound delay carries over to the next departure, and even less to the subsequent arrival. This indicates that 80–90% of delay shocks are absorbed through ground buffers, turnaround practices, and en-route adjustments. These findings confirm that European carriers operate schedules that are resilient to modest shocks, although tight utilisation patterns still leave limited room for recovery when larger disruptions occur.

Third, the environmental consequences of airborne delays are significant. Model 3 demonstrates that each extra airborne minute increases fuel burn by approximately 22 kg and CO_2 emissions by 71 kg on average. Conversely, negative airborne delays lead to proportionally lower fuel use. These effects primarily reflect actual changes in airborne duration—such as holding, rerouting, or weather-related inefficiencies—rather than deliberate speed-ups, whose net influence on fuel consumption is comparatively small.

Overall, the results highlight a clear operational–environmental trade-off: although airlines can partially buffer disruptions, the mechanisms available in the short run—especially en-route adjustments—carry measurable fuel and emissions costs.

5.2 Policy Implications

Three implications follow for policymakers and industry stakeholders.

First, improving schedule realism and buffer allocation can deliver both punctuality and environmental benefits. Since only a small fraction of delays can be mitigated within a flight, reducing the incidence of large departure disruptions is essential. More flexible sequencing, efficient ground-handling practices, and dynamic slot management would enhance recovery margins and reduce the fuel-intensive airborne inefficiencies identified in Model 3.

Second, environmental regulation, particularly within the EU Emissions Trading Scheme, could explicitly incorporate the operational sources of emissions. Because airborne delays mechanically increase fuel burn, integrating delay performance into environmental metrics would better align incentives toward punctual and fuel-efficient operation.

Third, stronger operational coordination between airlines and air navigation service providers could help stabilise daily operations and limit the need for fuel-intensive airborne adjustments. The estimates presented in this paper offer a foundation for assessing the potential benefits of such coordination in terms of both punctuality and emissions.

5.3 Limitations and Future Research

Two main limitations should be acknowledged. First, the analysis does not incorporate high-resolution trajectory or vertical-profile data, limiting the ability to disentangle operational speed-ups from meteorological factors such as wind fields and ATC-imposed rerouting. Second, the absence of detailed weather variables restricts the interpretation of airborne delay components, especially for cases where negative airborne delay results from tailwinds rather than mitigation behaviour.

One avenue for future work is to integrate trajectory-based ADS-B data and high-frequency meteorological information with the current dataset in order to better disentangle operational adjustments-such as speed changes arising from reroutings or ATC-initiated shortcuts-from non-operational drivers of airborne time. Finally, incorporating measures of passenger welfare and airline cost data would allow a more complete assessment of the economic and environmental trade-offs associated with delay management.

6 Appendix

Table 8: List of Countries Included in the Sample

Country Code	**Country Name**
IT	Italy
DE	Germany
FR	France
PT	Portugal
ES	Spain
NL	Netherlands
MT	Malta
IE	Ireland
DK	Denmark
CY	Cyprus
AT	Austria
SE	Sweden
FI	Finland
BE	Belgium
LU	Luxembourg
CH	Switzerland

Table 9: List of Airlines Included in the Sample

Airline Code	**Airline Name**
EI	Aer Lingus
XZ	AeroItalia
BT	Air Baltic Corporation
EN	Air Dolomiti
UX	Air Europa
AF	Air France
KM	Air Malta
OS	Austrian Airlines
NT	Binter Canarias
SN	Brussels Airlines
PM	Canaryfly
DE	Condor Flugdienst
XR	Corendon Airlines Europe
CY	Cyprus Airways
LH	Lufthansa
4Y	EW Discover
U2	Easyjet
EW	Eurowings
AY	Finnair
AZ	ITA Airways
IB	Iberia
KL	KLM-Royal Dutch Airlines
LG	Luxair
D8	Norwegian
DY	Norwegian Air Shuttle
FR	Ryanair
SK	SAS Scandinavian Airlines
SP	SATA Air Acores
S4	SATA International-Azores Airlines S.A.
TP	TAP Air Portugal
TB	TUI fly Belgium
OR	TUI fly Netherlands
X3	TUIfly
HV	Transavia
TO	Transavia France
T7	Twin Jet
V7	Volotea
VY	Vueling Airlines
W6	Wizz Air
W4	Wizz Air Malta

References

Brueckner, J. K. (2002a). Airport congestion when carriers have market power. *American Economic Review*, 92(5):1357–1375.

Brueckner, J. K. (2002b). Internalization of airport congestion. *Journal of Air Transport Management*, 8(3):141–147.

Brueckner, J. K. (2005). Internalization of airport congestion: A network analysis. *International Journal of Industrial Organization*, 23(7-8):599–614.

Brueckner, J. K., Czerny, A. I., and Gaggero, A. A. (2021). Airline mitigation of propagated delays via schedule buffers: Theory and empirics. *Transportation Research Part E: Logistics and Transportation Review*, 150:102333.

Brueckner, J. K., Czerny, A. I., and Gaggero, A. A. (2022). Airline delay propagation: A simple method for measuring its extent and determinants. *Transportation Research Part B: Methodological*, 162:55–71.

Brueckner, J. K., Czerny, A. I., and Gaggero, A. A. (2025). Gauging the effectiveness of airline schedule buffers in reducing arrival delays. *Journal of Air Transport Management*, 125:102776.

Bubalo, B. and Gaggero, A. A. (2021). Flight delays in european airline networks. *Research in Transportation Business & Management*, 41:100631.

Chen, Z., Wanke, P., Antunes, J. J. M., and Zhang, N. (2017). Chinese airline efficiency under co2 emissions and flight delays: A stochastic network dea model. *Energy Economics*, 68:89–108.

Dissanayaka, D., Adikariwattage, V., and Pasindu, H. (2020). Evaluation of co emission from flight delays at taxiing phase in bandaranaike international airport (bia). *Transportation Research Procedia*, 48:2108–2126.

Dou, L., Kastl, J., and Lazarev, J. (2024). Quantifying delay propagation in airline networks.

Forbes, S. J., Lederman, M., and Yuan, Z. (2019). Do airlines pad their schedules? *Review of Industrial Organization*, 54:61–82.

Huang, F., Zhou, D., Hu, J.-L., and Wang, Q. (2020). Integrated airline productivity performance evaluation with co2 emissions and flight delays. *Journal of Air Transport Management*, 84:101770.

Kafle, N. and Zou, B. (2016). Modeling flight delay propagation: A new analytical-econometric approach. *Transportation Research Part B: Methodological*, 93:520–542.